Atmospheric Environment 107 (2015) 70–84

Contents lists available at ScienceDirect

Atmospheric Environment

journal homepage: www.elsevier.com/locate/atmosenv

Long-term NO_x trends over large cities in the United States during the great recession: Comparison of satellite retrievals, ground observations, and emission inventories

Daniel Q. Tong [a, b, c, *], Lok Lamsal [d, e], Li Pan [a, b], Charles Ding [a, f], Hyuncheol Kim [a, b], Pius Lee [a], Tianfeng Chai [a, b], Kenneth E. Pickering [e], Ivanka Stajner [g]

[a] NOAA Air Resources Laboratory (ARL), NOAA Center for Weather and Climate Prediction, 5830 University Research Court, College Park, MD 20740, USA
[b] Cooperative Institute for Climate and Satellites, University of Maryland, College Park, MD 20740, USA
[c] Center for Spatial Information Science and Systems (CSISS), George Mason University, Fairfax, VA 22030, USA
[d] Goddard Earth Sciences Technology and Research, Universities Space Research Association, Columbia, MD, USA
[e] NASA Goddard Space Flight Center, Greenbelt, MD, USA
[f] University of California at Berkeley, Berkeley, CA, USA
[g] NOAA National Weather Service, Silver Spring, MD 20910, USA

HIGHLIGHTS

- Derived multi-year urban NOx trend from satellite (OMI) and ground observations (AQS).
- Revealed NOx responses to the 2008 Economic Recession by OMI and AQS.
- The trend not well captured by emissions used for national air quality forecasting.
- Demonstrated how to use space and ground observations to evaluate emission updates.

ARTICLE INFO

Article history:
Received 11 April 2014
Received in revised form
2 January 2015
Accepted 14 January 2015
Available online 15 January 2015

Keywords:
NO_x
Emission
Trend
Air quality forecast
Recession
OMI NO2
Ozone
AQS
NAQFC

ABSTRACT

National emission inventories (NEIs) take years to assemble, but they can become outdated quickly, especially for time-sensitive applications such as air quality forecasting. This study compares multi-year NO_x trends derived from satellite and ground observations and uses these data to evaluate the updates of NO_x emission data by the US National Air Quality Forecast Capability (NAQFC) for next-day ozone prediction during the 2008 Global Economic Recession. Over the eight large US cities examined here, both the Ozone Monitoring Instrument (OMI) and the Air Quality System (AQS) detect substantial downward trends from 2005 to 2012, with a seven-year total of −35% according to OMI and −38% according to AQS. The NO_x emission projection adopted by NAQFC tends to be in the right direction, but at a slower reduction rate (−25% from 2005 to 2012), due likely to the unaccounted effects of the 2008 economic recession. Both OMI and AQS datasets display distinct emission reduction rates before, during, and after the 2008 global recession in some cities, but the detailed changing rates are not consistent across the OMI and AQS data. Our findings demonstrate the feasibility of using space and ground observations to evaluate major updates of emission inventories objectively. The combination of satellite, ground observations, and in-situ measurements (such as emission monitoring in power plants) is likely to provide more reliable estimates of NO_x emission and its trend, which is an issue of increasing importance as many urban areas in the US are transitioning to NO_x-sensitive chemical regimes by continuous emission reductions.

1. Introduction

Nitrogen oxides (NO_x = NO + NO_2) are key precursors to tropospheric ambient ozone (O_3) and fine particulate matter ($PM_{2.5}$) (Crutzen and Gidel, 1983; Spicer, 1983), which has been

* Corresponding author. NOAA Air Resources Laboratory (ARL), NOAA Center for Weather and Climate Prediction, 5830 University Research Court, College Park, MD 20740, USA.
E-mail address: Daniel.Tong@noaa.gov (D.Q. Tong).

http://dx.doi.org/10.1016/j.atmosenv.2015.01.035

associated with adverse health effects, including respiratory diseases and cardiovascular mortality (Pope et al., 2002; Jerrett et al., 2009). As of December 2013, the United States Environmental Protection Agency (US EPA) estimates that more than one-third of the US population lives in areas that exceed the national ambient air quality standards (NAAQS) for either O_3 or $PM_{2.5}$ (US EPA, 2014a, 2014b). To assist state and local agencies in mitigating the effects of unhealthy levels of air pollution, the National Air Quality Forecasting Capability (NAQFC) system (Otte et al., 2005), currently operated by the National Weather Service, was designed to provide air quality forecasting guidance over the contiguous United States, Hawaii, and Alaska for next day forecasts (Stajner et al., 2012). NO_x are emitted from both anthropogenic sources (transportation, power plants, and fertilizers) and natural sources (biomass burning, lightning, and soils) (Warneck, 2000). Once emitted, NO_x reacts with volatile organic compounds under sunlight to form tropospheric ozone (Liu et al., 1987) and particulate nitrate, an important component of $PM_{2.5}$. Hence, quantifying the amount of NO_x emitted into the atmosphere is essential for reliable prediction of surface ozone and $PM_{2.5}$.

It is often challenging to provide accurate estimates of NO_x emissions for time-sensitive applications such as NAQFC, given the rapid progression of emission control and other socioeconomic events that affect emission loading (e.g., Harley et al., 2005; van der A et al., 2008; Stavrakou et al., 2008; Konovalov et al., 2010; Pinder et al., 2011; Castellanos and Boersma, 2012; Duncan et al., 2013). NAQFC relies on national emission inventories (NEIs) to account for thousands of anthropogenic emission sources and other emission models for natural sources. The substantial cost and effort entailed in collecting data relevant for compiling NEIs are prohibitive for frequent and timely updates of NO_x NEIs using conventional emission modeling approaches. As a result, the emission data used in NAQFC are several years behind the forecasting year, imposing uncertainties on air quality forecasting (Tong et al., 2012).

Can satellite-based emission data provide reliable information in order to rapidly update NO_x emission inventories and thereby support NAQFC-type air quality applications? NO_2 retrievals from polar orbiting satellite sensors such as SCIAMACHY and GOME have been used to update anthropogenic NO_x emission inventories (Martin et al., 2003; Lamsal et al., 2011; Mijling and van der A, 2012). This satellite-based approach, while showing great potential to reduce the emission time lag, has yet to be verified with independent data sources. To evaluate the robustness of this approach, this study thus compares the long-term NO_2 trends derived from the Ozone Monitoring Instrument (OMI) (Boersma et al., 2007) with the operational emission data used in NAQFC predictions, with emphasis on both the emission changes between major updates and the year-to-year progression over eight metropolitan areas from 2005 to 2012. A third data source, the EPA's AQS ground observations, serves as an independent reference to help verify urban NO_x trends. Estimation of future year emissions for air quality and climate modeling often relies on emission projections (Bond et al., 2004; Granier et al., 2011). NAQFC emissions are updated annually based on the available emission inventories, emission measurements, and projections. Rigorous evaluations of these annual updates, however, have not been performed regularly, largely because of the lack of observational data to directly verify emission projections. Meanwhile, AQS data have been used as a proxy for urban emissions since morning rush-hour concentrations are predominantly influenced by emissions from heavy commuter traffic (Godowitch et al., 2010). The AQS measurements have been coupled with other data to identify source strength and the origin of reactive nitrogen oxides over the Southeastern United States (Tong et al., 2005). Therefore, all three data sources provide independent quantification of NO_x emissions that can be compared over a fixed time period.

The intercomparisons of changes in NO_x from NAQFC, OMI, and AQS are expected to serve dual purposes: 1) to compare the NO_x trends derived from space and ground observations; and 2) to evaluate NAQFC emission updates against satellite and ground observations. We focus here on the NO_x trends over eight major metropolitan areas (Fig. 1) where NO_x emission density is high and AQS monitors are abundant. We further concentrate on the NO_x trends during summertime when the NO_x photochemical lifetime is shorter (4 h at noon), the carryover from the previous day is limited and regional transport is at minimal, yielding a column that is especially representative of local surface emissions (Russell et al., 2010). Further, the number of available satellite measurements is maximized during summer months, when cloud cover is lowest. Finally, these studied areas are among the most populous cities in

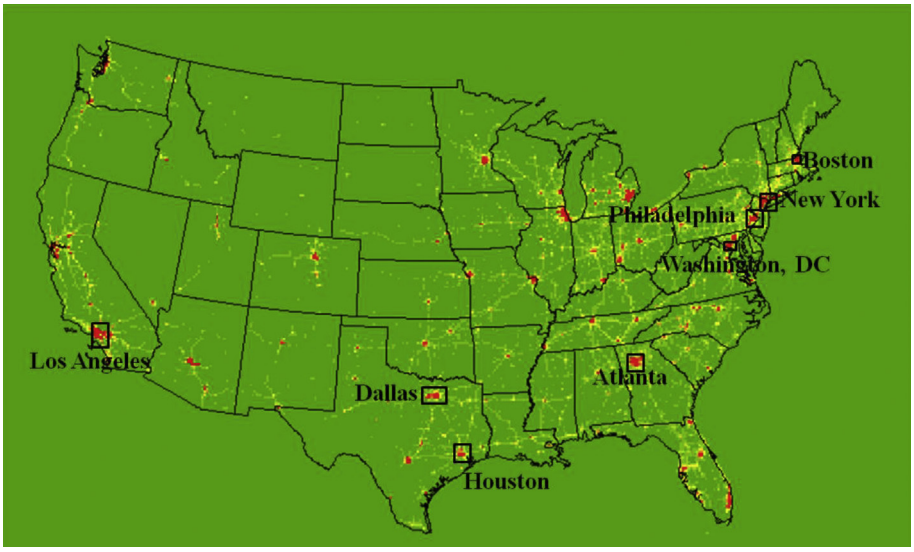

Fig. 1. Locations of the eight selected metropolitan statistical areas, which are among the most densely populated cities in the United States. The background color represents NO_x emission density based on the NAQFC emission data, with red indicating high NO_x emission density. (For interpretation of the references to color in this figure legend, the reader is referred to the web version of this article.)

the United States, where elevated O_3 and $PM_{2.5}$ levels pose particular health concerns.

2. Data sources and method

2.1. NAQFC NO_x emissions

The NAQFC system uses the Community Multiscale Air Quality (CMAQ) model (Byun and Schere, 2006) to provide next-day prediction of surface O_3 concentrations over 50 US states. Inputs to the CMAQ model include emission data processed from NEIs and hourly meteorological data from NOAA's operational North American Mesoscale (NAM) meteorological model (Otte et al., 2005; Lee and Fong, 2011; Stajner et al., 2012). The NAM relies on the meteorology dynamic core of WRF-NMM (Nonhyrostatic Mesoscale Model) on the B grid (WRF-NMMB) with upgraded tracer advection scheme. A post-processor has been used to convert NAM meteorology data from a rotated latitude–longitude map projection on an Arakawa-B staggering grid to a Lambert conformal map projection on an Arakawa-C staggering grid with a 12 km horizontal resolution. The historic emission data used by NAQF is a key input and is summarized below. The NAQFC emission dataset includes gaseous and particulate emissions from anthropogenic sources (area, mobile, and point) and natural sources (biogenic, soil, and sea salt). Since the contribution of natural sources to urban NO_x emissions is small, we emphasize here the emission inventories of area, mobile, and point sources.

NAQFC operational O_3 prediction has been expanded to cover the entire continental United States in 2007 (Eder et al., 2009; Kang et al., 2010; Tong et al., 2007), for which the US EPA 2005 NEI version 1 (NEI05v1) is used for US sources, 1999 Mexico NEIs for Mexico, and 2000 Environmental Canada Emission Inventories for Canada. The EPA Office of Transpiration and Air Quality 2005 on-road emission inventories are used to generate mobile NO_x emissions over the United States. NEI05v1 data are also used as the base inventories for the area sources and the point sources of electricity-generating units (EGUs) and non-EGUs in the US. The emission inventories are assembled and checked for consistency and replication. The emission sources that are not subject to meteorological changes, including area and mobile source inventory data are further processed using an emission tool called Sparse Matrix Operator Kennel Emission (SMOKE) (Houyoux et al., 2000) to represent monthly, weekly, daily, and holiday/non-holiday variations that are specific for each year (Otte et al., 2005). For those sources that are affected by meteorology, including power plants and biogenic sources, the emission data are generated dynamically using real-time weather forecasting data using a preprocessor called PREMAQ (Otte et al., 2005).

NAQFC emissions are updated each spring before the beginning of the so-called “ozone season” (May to September) once reliable emission data have been made available. To ensure the stability and continuity of forecasting operations, NAQFC adopts only well-proven emission data that both reflect improved emission science and contribute positively to forecast performance. One such update is carried out for the EGU sector. NO_x emissions from US electricity generation units (EGUs) sources are upgraded by using the US EPA Continuous Emission Monitoring data, which are usually two years behind the forecasting year. Therefore, the US Department of Energy Annual Energy Outlook (US DOE, 2012), released in early spring each year, is used to project EGU emissions to the forecasting year based on the two-year forecasted growth in regional energy usage.

Major updates were performed in 2012 for the US and Canadian sources (Pan et al., 2014). The US off-road emissions in the 2005 NEI were replaced with the projected emission data (version 2012cs) prepared for the Cross-State Air Pollution Rule (CSAPR) (US EPA, 2011). This data is comprised of a run of the National Mobile Inventory Model (NMIM) estimates that utilized the NR05d-Bond-final version of the NONROAD model to project emissions for 2012 based on future-year population estimates and control programs. US mobile source emissions from the 2005 NEIs were scaled down by using the CSAPR 2005–2012 emission projection factors. The CSAPR projection for mobile sources was derived from the MOtor Vehicle Emission Simulator (MOVES) version 2010 run for NMIM 2012 estimates. Aggregated state-level data from the CSAPR run were used in the subsequent emission projection. The projected 2012 scenario represents the best estimate for future years without the implementation of remedy controls for EGUs (US EPA, 2011). This exclusion is not an issue for this study since EGU emissions are treated here separately with updated data sources.

2.2. OMI NO_2 observations

The OMI aboard the Aura satellite is a nadir-viewing hyperspectral imaging spectrometer that measures the solar backscattered radiance and the solar irradiance in the ultraviolet and visible regions (270–500 nm) (Levelt et al., 2006). The Aura spacecraft was launched on 15 July 2004 into a sun-synchronous polar orbit with a local equator-crossing time of 13:45 h in the ascending node. The OMI views the Earth along the satellite track with a swath of 3600 km on the surface in order to provide daily global coverage. In the normal global operational mode, the OMI ground pixel at nadir is approximately 13 km $\times$ 24 km, with increasing pixel sizes toward the edges of the orbital swaths.

Here, we use the OMI standard product (version 2.1, collection 3) described by Bucsela et al. (2013) and available from the NASA Goddard Earth Sciences Data Active Archive Center (http://disc.sci.gsfc.nasa.gov). The NO_2 retrieval algorithm employs the Differential Optical Absorption Spectroscopy (DOAS) technique (Platt, 1994; Boersma et al., 2007) to quantify NO_2 abundance (slant column) by using the nonlinear least squares fitting of modeled spectrum to the OMI-measured attenuation spectra in a 405–465 nm window. The slant column represents the integrated abundance of NO_2 along the average photon path from the sun, through the atmosphere, to the satellite. The measured slant column densities (SCDs) are corrected for instrumental artifacts (stripes) (Dobber and Braak, 2010) by using the cross-track variation of the stratospheric air mass factor (AMF). AMFs are calculated by using a look-up table of vertically resolved NO_2 sensitivities (scattering weights) and various input parameters including viewing geometry, surface reflectivity, cloud pressure, cloud radiance fraction, and *a priori* NO_2 vertical profile shapes. To separate stratospheric and tropospheric components, the algorithm applies stratospheric AMFs to de-striped SCDs in order to yield initial vertical column densities (VCDs). Areas of tropospheric contamination in the stratospheric NO_2 field are identified by using the monthly mean tropospheric NO_2 columns from a Global Modeling Initiative (GMI) simulation. Those regions are then masked, and the residual field of the stratospheric vertical column densities VCDs measured outside the masked regions, primarily from unpolluted or cloudy areas, is smoothed by using a boxcar average and a 2D interpolation scheme to estimate the stratospheric NO_2 columns for each measurement.

The retrieval of the tropospheric vertical NO_2 column is sensitive to the *a priori* NO_2 vertical profile shapes, which are used in the calculation of the tropospheric AMF. In this work, we follow the approach in Lamsal et al. (2015) by using the scattering weights and high resolution NO_2 vertical profiles ($0.5^\circ \times 0.67^\circ$) provided by the nested grid GEOS-Chem simulation to recompute the AMF and OMI tropospheric NO_2 columns. The high resolution NO_2 profiles improve the representation of vertical distributions within OMI

pixels.

The errors in the retrieval of tropospheric NO_2 columns arise from errors in the SCD, in the separation of stratospheric and tropospheric components, and from the AMF calculation (Boersma et al., 2004). The uncertainty due to spectral fitting and the stratosphere–troposphere separation dominates the overall error over clean areas. AMF errors dominate overall errors in cloudy and polluted areas. The estimated error in tropospheric NO_2 columns under cloudy conditions is significantly higher at ~60% compared with ~30% errors under clear-sky conditions (Martin et al., 2002; Boersma et al., 2007 Bucsela et al., 2013). The OMI tropospheric NO_2 retrievals agree within 20% with the ground-based and in-situ NO_2 measurements (Lamsal et al., 2015), and MAX-DOAS measurements from aircraft (Oetjen et al., 2013).

2.3. AQS ground observations

Ground NO_x measurements are obtained from the EPA AQS monitoring network. The AQS network collects ambient air pollution data from monitoring stations located in urban, suburban, and rural areas. Most AQS monitors determine NO_x concentrations by using the chemiluminescence instruments described by McClenny et al. (2002). Morning rush-hour means are calculated from quality-controlled hourly NO_x values for the hours 0600, 0700, 0800, and 0900 local time, following the observed temporal patterns for summertime weekday NO_x variations presented by Godowitch et al. (2010). These morning hours are associated with the highest NO_x concentrations contributed by both typical commuter traffic peaks and the shallow planetary boundary layer, making them an ideal indicator for assessing local emission conditions. The choice of the morning time period is expected to minimize chemical interference from secondary nitrogen species with NO_x measurements during the photochemically-active afternoon period (Dunlea et al., 2007). This advantage has been confirmed by a model comparison of the concentrations of NO_x and total nitrogen species (NO_y) in a 3D chemical transport model (Godowitch et al., 2010). The data used in this study are downloaded from the AQS online database (http://www.epa.gov/ttn/airs/airsaqs/detaildata/downloadaqsdata.htm).

2.4. Three-member intercomparison method

Long-term trends are derived from NAQFC, OMI, and AQS for 2005–2012 over eight large cities in the US, namely Atlanta, Boston, Dallas, Houston, Los Angeles, New York, Philadelphia, and Washington, DC. Averages are calculated for July each year by aggregating the data over time and space. NAQFC and AQS data have an hourly temporal resolution, while OMI data are measured in the early afternoon. Different approaches are used to define the spatial coverage of each city. A rectangular box is selected to represent the city in NAQFC by examining the spatial distribution of NO_x emissions (Fig. 1). The spatial coverage of this box is defined based on both geographical proximity to the urban center and the spatial distribution of the NO_2 plume or emission density. All NO_x monitors lying within this box are included in the AQS dataset for that city. For OMI, we include all cloud-filtered pixels that lie in or intercept with the rectangular box for each city, and an area-weighted average is used in the subsequent analysis.

Percentage changes for each year are determined as $(Y2 - Y1)/Y1 \times 100\%$. For the multi-year trend, the 2005 level is used as the baseline (Y1) to examine the changes. Early morning hours are chosen from NAQFC and AQS to assemble the monthly averages, as described above. We also compare the NO_x derived from early afternoon hours (12 pm–3 pm local time) that cover the OMI overpass time in order to examine how using different observing times affects the NO_x trends. While this approach leaves the rural areas unchecked, an earlier study by Lamsal et al. (2011) showed that over 90% of NO_x emissions are found in urban areas.

3. NAQFC NO_x emissions and O_3 prediction

3.1. NAQFC NO_x emission trends

Although the emissions from various sectors have been updated on an annual basis, the 2012 update is by far the largest and most relevant emission change for urban emissions. Fig. 2 shows the monthly mean NO_x emission rates in July 2011 and July 2012 and the difference between these two years over the continental United States. Until 2012, the 2005 emission inventories were used to generate operational NAQFC emissions with the exception of point source emissions. The point source updates contribute up to 5% change per year to NAQFC NO_x emission data, but have little impact on urban NO_x emissions since most EGUs are located outside populous areas (Frost et al., 2006).

Fig. 2a shows that urban sources dominate NO_x emissions over the continental United States, confirming the importance of urban NO_x. High emission density is also found at scattered places (locations of power plants or large industrial boilers) and, to a lesser extent, along major highways. The updated NO_x emissions (Fig. 2b) resemble the old dataset in spatial distribution (with dominant urban emissions), but the magnitude of emission changes varies from place to place. Because on-road and off-road engine emissions, which account for approximately 60% of US NO_x emissions, tend to occur in or near urban centers, the NO_x changes (Fig. 2c) are also seen at these locations. Therefore, examining urban NO_x emission changes will allow us to capture the most important changes in NO_x emissions.

3.2. Effects on NAQFC O_3 prediction

Implementation of the 2012 emission updates in the NAQFC system has improved O_3 prediction considerably (Pan et al., 2014). NAQFC O_3 forecasting long suffered the issue of overprediction (e.g., Eder et al., 2009; Tong et al., 2009; Chai et al., 2013; Pan et al., 2014), largely because of the rapid emission reduction caused by emission controls and the economic recession (Russell et al., 2012), which were not included in NAQFC emission updates. The 2012 emission updates have reduced both O_3 and NO_x biases compared with ground observations that were made during the NASA Earth Venture–1 DISCOVER-AQ (Deriving Information on Surface Conditions from Column and Vertically Resolved Observations Relevant to Air Quality) field campaign in Maryland (Pan et al., 2014). The one-month comparison shows that the NAQFC air quality model predictions of NO_x and O_3 concentrations have improved over the entire continental US.

We examine here the performance of multi-year NAQFC operational O_3 prediction (2009–2012) (Fig. 3). In all years before the 2012 update, NAQFC overpredicts surface O_3 concentrations in the ozone season, with a larger discrepancy during the summertime when the exceedance of the NAAQS for O_3 is more frequent. Although meteorological conditions vary from year to year, this recurring overprediction suggests that the emission data, particularly NO_x emissions, are likely to be a major contributing factor to the model bias. Comparisons against ground and satellite observations also confirmed that NAQFC tends to overestimate NO_2 surface concentration and column density before the 2012 updates (Choi et al., 2012; Chai et al., 2013). After the 2012 updates, the reduced NO_x emissions resulted in considerable improvements in O_3 prediction performance (see the last panel in Fig. 3).

We further quantify O_3 prediction performance against observations using two statistical metrics in Fig. 4. The mean bias (MB) is

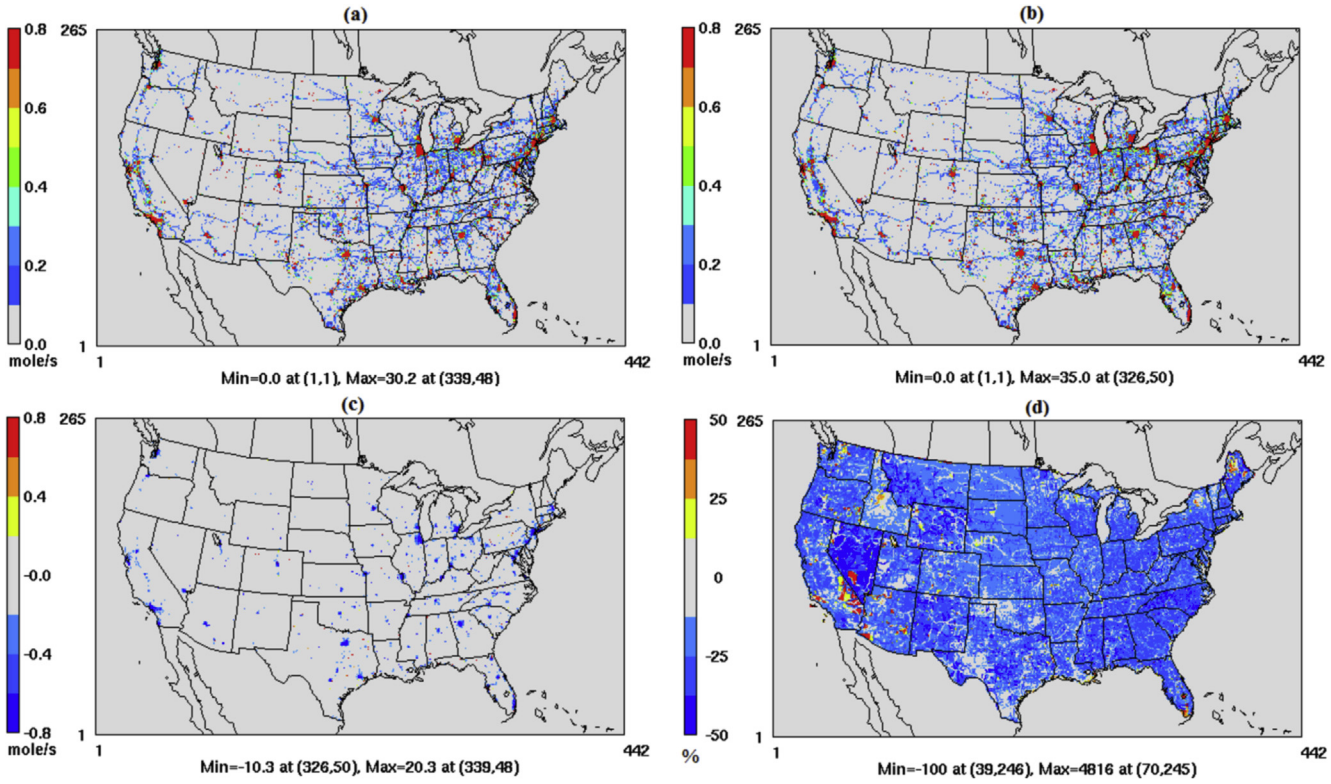

Fig. 2. NAQFC NO_x emissions before (a) and after (b) the 2012 major updates and their difference (2012 minus 2005) in emission rate (c) and percentage (d) during summertime (July).

the mean difference between predicted and observed (model minus observation) values. The root mean square error (RMSE) reflects the absolute difference between the model and observational values. It describes the model bias from a different angle (i.e., it avoids the possibility of positive and negative biases canceling each other) (Tong and Mauzerall, 2006). From 2009 to 2011, the bias is relatively small during springtime, and then it grows larger in the warm season, reaching up to 10 ppbv during summertime. The RMSE is considerably higher than the mean bias in springtime, suggesting that the relatively low bias is partially caused by the canceling of positive and negative biases. The two statistics match better in summer, when both values are higher. The concurrent high values in both statistics indicate that positive biases dominate during summertime. After the 2012 update, both the mean bias have been reduced in the summer by 3–10 ppbv for the daily maximum 8-h O_3 concentrations (see additional discussion in the SI). The summertime RMSE was around 14 ppbv before 2012 and dropped to around 11 ppbv after 2012. While the evaluation covers all monitoring stations in the continental United States, we further examine the model performance at the eight metropolitan areas. Overall cities, the 2012 emission updates have reduced summertime O_3 biases, although the magnitude of performance improvement varies from city to city. This improved model performance suggests that the emission update has generally captured the downward trend in NO_x emissions over the continental United States. However, the extent to which this update has reflected the magnitude of the NO_x changes remains unclear. To evaluate the emission projection implemented in NAQFC, we examine the NO_x change observed from the space and ground monitors.

4. Satellite-observed NO_2 trend from 2005 to 2012

Fig. 5 demonstrates a rapid change in tropospheric NO_2 columns between 2005 and 2012 above North America. We observe a NO_2 reduction of up to 50% over this period, with a large absolute reduction in the polluted regions of the country including the eastern US, Los Angeles, and Chicago. In contrast, OMI shows a small increase in NO_2 over the rural regions of the central US because of interannual variations in soil NO_x emissions (Hudman et al., 2012). The trends in NO_2 vary over time, with the large annual rate of decrease larger for 2005–2009 than for 2009–2011. These NO_2 reductions are primarily due to environmental regulations and technological improvements, as well as the economic recession (Russell et al., 2012).

Here, we focus on comparing the trends derived from the OMI tropospheric NO_2 columns with those from ground-based NO_2 observations and NAQFC NO_x emission data over the selected urban areas. To examine the changes in the OMI tropospheric NO_2 columns over these locations, we identify coincident OMI measurements each day. To ensure similar spatial sampling, we exclude the ground pixels at swath edges with pixel sizes larger than 50×24 km^2 as well as those affected by row anomaly. We include cloud-free scenes with a cloud radiance fraction <0.5 in order to reduce retrieval errors. Annual averages are calculated from area-weighted monthly averages of the OMI tropospheric NO_2 columns.

5. Comparison of OMI, AQS, and NEI trends

5.1. Comparison of interannual variations

In this section, we compare the NO_x trends from NAQFC, OMI, and AQS over the eight cities from 2005 to 2012 (Fig. 6). We focus on two aspects of the trends: the annual changes and the overall change during the seven-year period. As the same base NEIs were used to generate the operational NAQFC emission data, it is no surprise that there was little change over major urban centers until

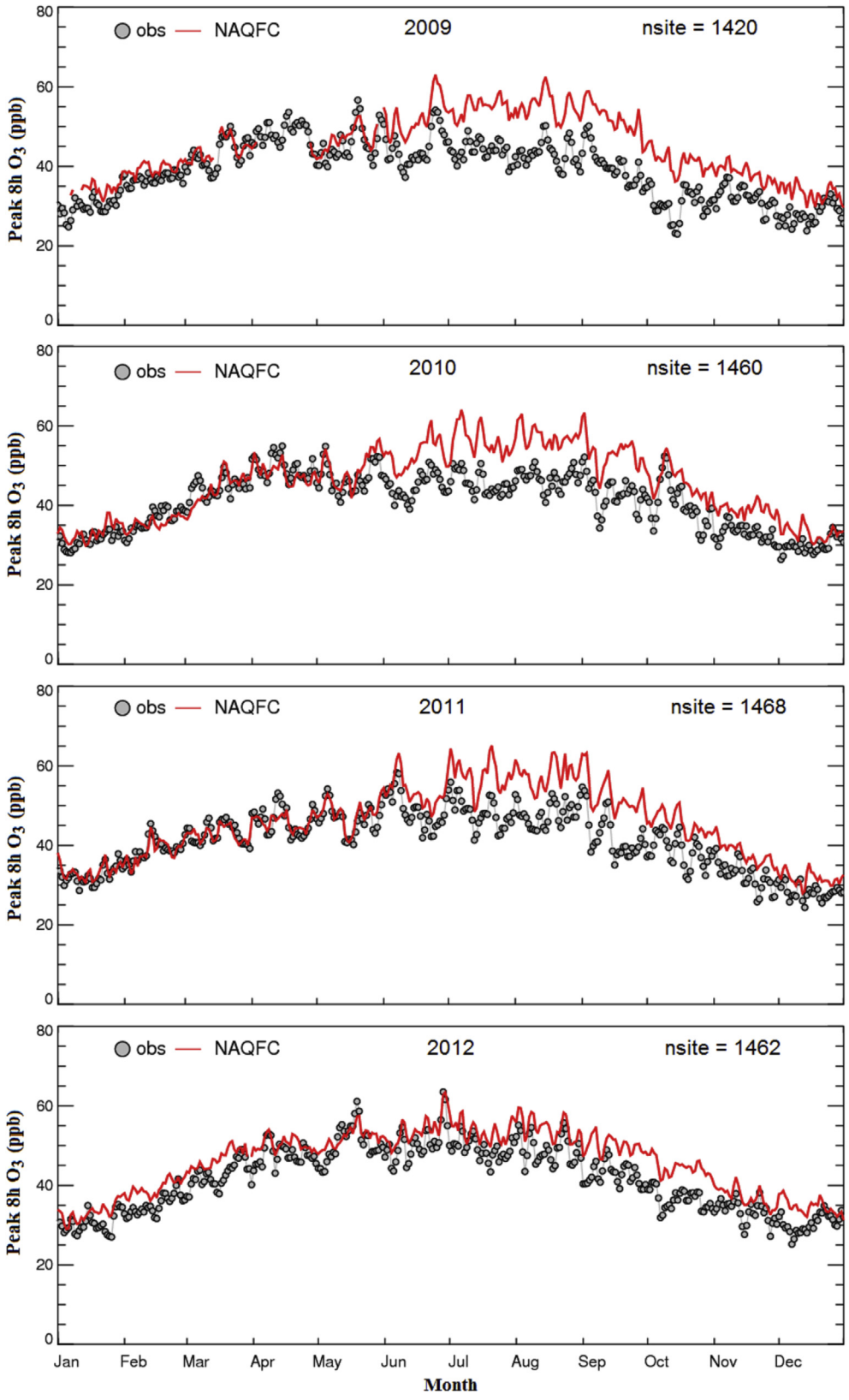

Fig. 3. Comparisons of the daily maximum 8-h O_3 concentrations from NAQFC predictions (red solid line) and ground monitor observations from the AQS network (dotted line) over the continental United States from 2009 to 2012. (For interpretation of the references to color in this figure legend, the reader is referred to the web version of this article.)

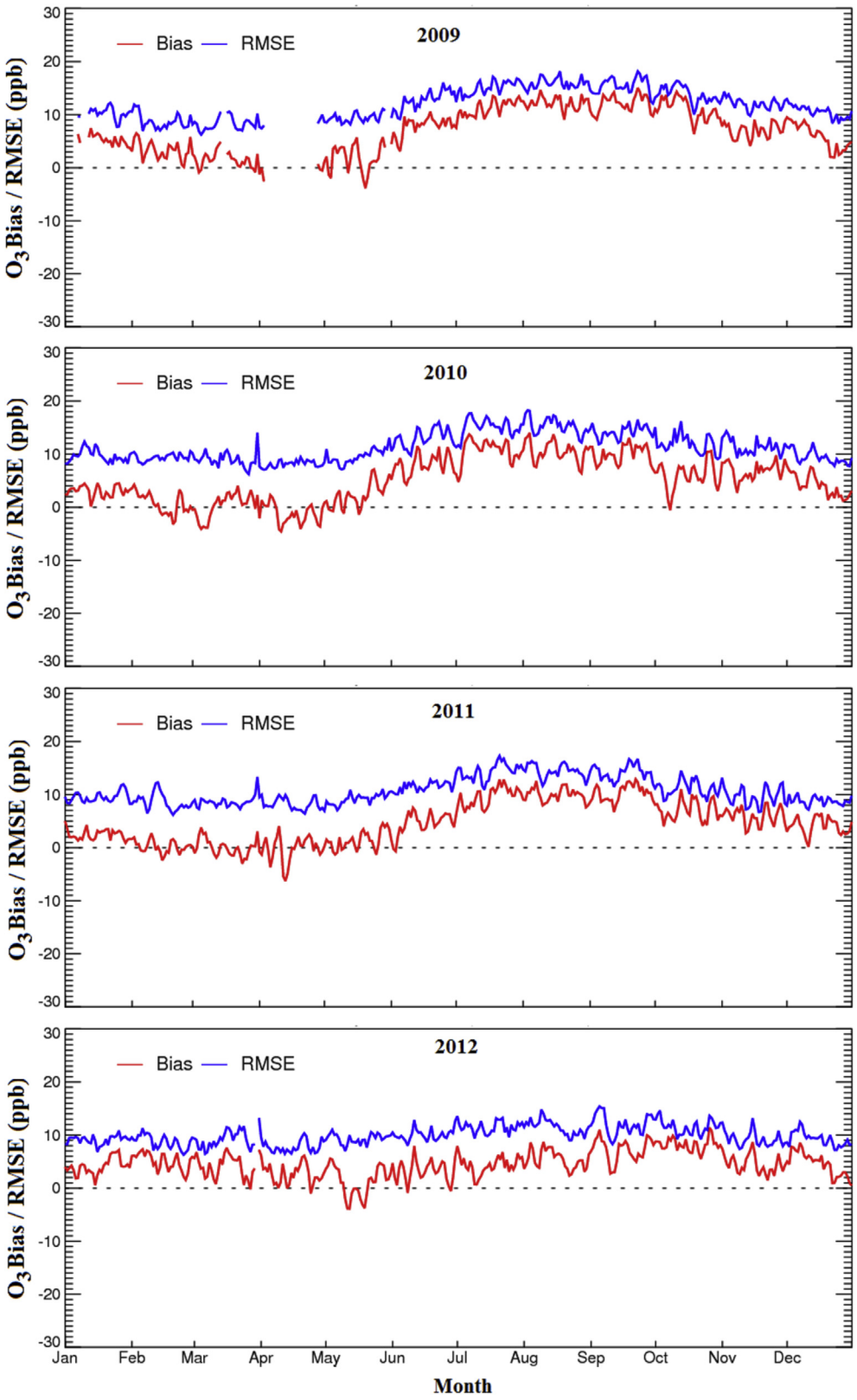

Fig. 4. The mean bias and RMSE of the NAQFC predicted daily maximum 8-h O_3 concentrations compared with the ground measurements at the AQS network from 2009 to 2012.

2012. Meanwhile, OMI and AQS show continuous changes in NO_x in all cities. Although NAQFC point source emissions were updated annually with CEMs and DOE projections, these updates have little impact on urban NO_x emissions. Below, we compare the multi-year NO_x trends from the three data sources for each city.

5.1.1. Atlanta

NAQFC estimates a 31% reduction in NO_x emissions from 2005 to

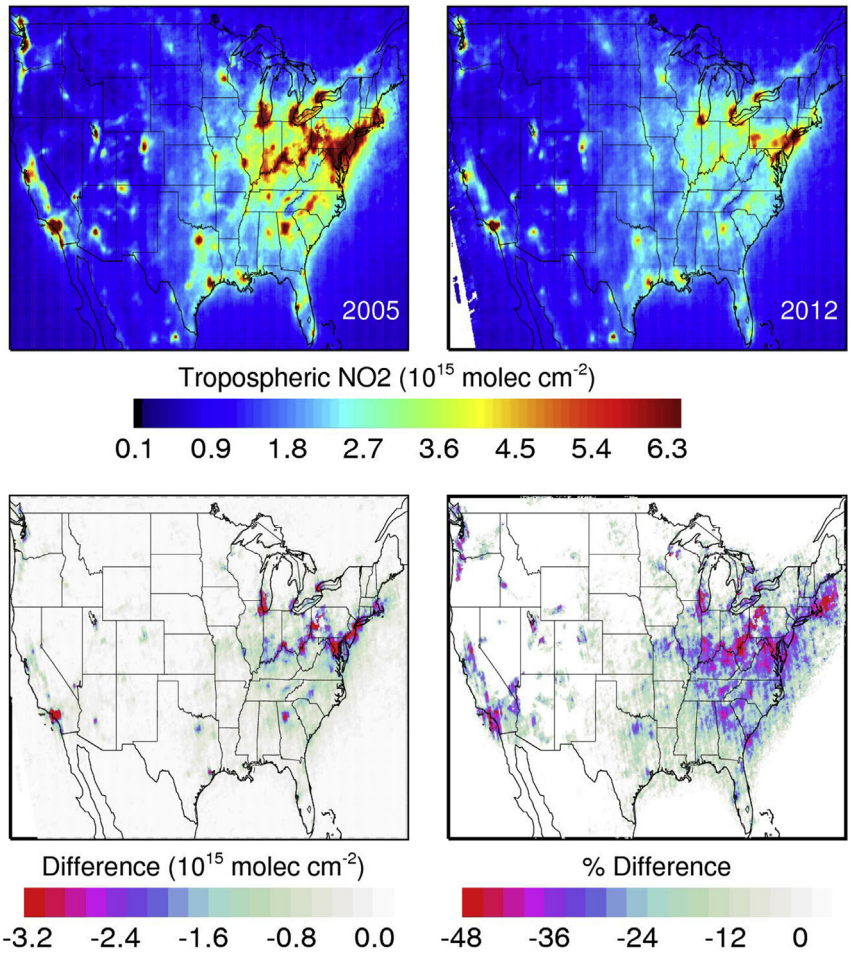

Fig. 5. NASA OMI NO_2 retrievals over North America in 2005 and 2012 during which a large NO_2 reduction was observed. Upper plates display NO_2 column in 2005 (left) and 2012 (right) and the lower plates show the NO_2 difference between 2005 and 2012 in vertical column density (left) and percentage (right).

2012 in Atlanta, with a 38% decrease in mobile source emissions and a 13% decrease in area source emissions. Both OMI and AQS display a larger reduction than NAQFC (Fig. 6a). The OMI and AQS trends generally agree with each other within a ±5% range except for 2006 and 2009. OMI shows a monotonic and gradual reduction through the entire period, while AQS shows almost no change from 2005 to 2006 but a remarkable dive from 2006 to 2009. Little change in AQS occurred between 2009 and 2012. The mean changing rates of NO_2 over Atlanta are −6.0%/yr, −6.4%/yr and −4.4%/yr from OMI, AQS and NAQFC, respectively.

5.1.2. Boston

Over Boston, all three data sources show a closely matched overall change, with 28%, 37%, and 33% decreases from the 2005 level according to NAQFC, OMI, and AQS, respectively (Fig. 6b). These datasets, however, differ in the sequence of NO_x changes. OMI displays a continuously decreasing trend in the entire period except the final two years, while AQS shows a small decrease in the first half of the period and then a sharp downward trend in the second. Among the eight cities investigated here, Boston sees the largest variability in the year-to-year change between OMI and AQS. The mean changing rates of NO_2 are −5.3%/yr, −4.7%/yr and −4.0%/yr from OMI, AQS and NAQFC, respectively.

5.1.3. Dallas

Good agreement is seen among the trends over Dallas, with a close match of both the overall change and annual change between OMI and AQS. The OMI and AQS trends display consistent patterns in NO_x changes, with a slightly larger discrepancy in 2010 and 2011 before converging in 2012. The mean changing rates of NO_2 are −4.9%/yr, −4.7%/yr and −3.4%/yr from OMI, AQS and NAQFC, respectively.

5.1.4. Houston

Good agreement is also observed over Houston, except the noticeable discrepancy between OMI and AQS in the first half of the period. The overall changes are −28%, −24%, and −25% according to NAQFC, OMI, and AQS, respectively, a rare case in which the magnitude of the projected NO_x emission change in NAQFC is larger than the observed one. It should be pointed out, however, that these numbers are very close compared with those in other cities, suggesting that both OMI and AQS provide reliable observations of the NO_x trend in Houston. The early years, noticeably from 2006 to 2008, see a difference of up to 10% between OMI and AQS, which decreases after 2009 (<2%). The mean changing rates of NO_2 are −3.4%/yr, −3.6%/yr, and −4.0%/yr from OMI, AQS and NAQFC, respectively.

5.1.5. Los Angeles

The comparison of NO_x trends over Los Angeles shows a large difference in the overall changes between NAQFC emissions and the observations. NAQFC estimates a modest reduction of −15%, while

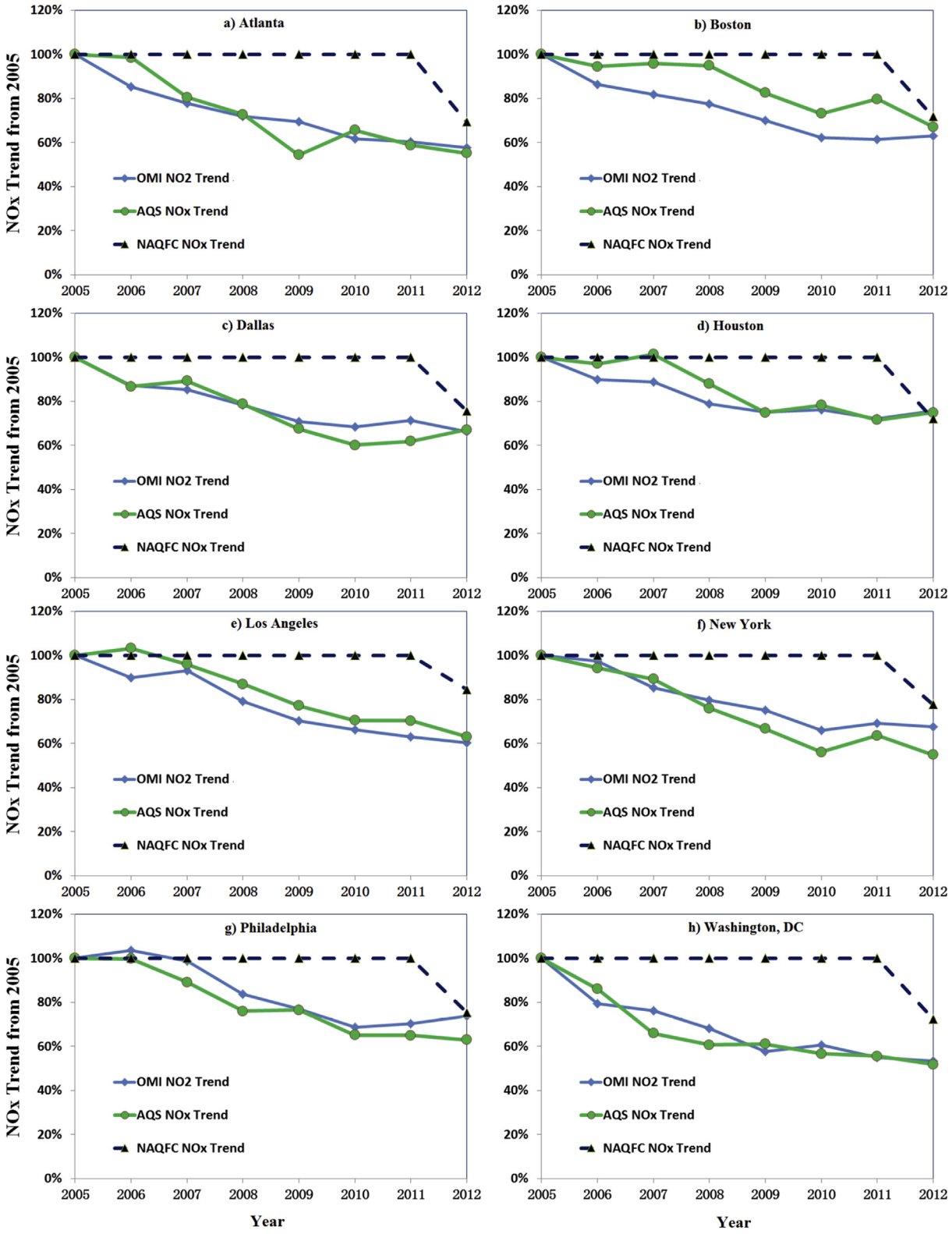

Fig. 6. Intercomparison of summertime (July) NO_x trends derived from OMI, AQS, and NAQFC from 2005 to 2012 over the eight studied cities: a) Atlanta, b) Boston, c) Dallas, d) Houston, e) Los Angeles, f) New York, g) Philadelphia, and h) Washington, DC.

OMI and AQS show −40% and −37% decreases between 2005 and 2012, respectively. In addition to the overall change, OMI and AQS generally agree with each other on the yearly trend except for 2006 in which opposite trends are observed. In other years, both OMI and AQS show a consistently downward trend. The mean changing rates of NO_2 are −5.7%/yr, −5.3%/yr and −2.1%/yr from OMI, AQS and NAQFC, respectively. The OMI and AQS changing rates are close to the mean NO_2 column growth rate (−5.07%/yr) from a multi-year

single-sensor analysis based on SCIAMACHY (Schneider and van der A, 2012). A similar changing rate (−5.8%/yr) was also derived from a multi-instrument fitting using the GOME, SCIAMACHY, OMI, and GOME-2 instruments (Hilboll et al., 2013). The large discrepancy among the NAQFC, OMI, and AQS trends suggests that the NAQFC emission projection over Los Angeles does not capture the magnitude of recent emission changes.

5.1.6. New York

Both OMI and AQS display larger NO_x reduction rates than NAQFC in New York: −32% according to OMI and −45% according to AQS compared with −22% from the data on NAQFC emissions. The mean changing rates of NO_2 are −4.6%, −6.4% and −3.1% from OMI, AQS and NAQFC, respectively. The OMI change is smaller than the AQS change in most years, but the two datasets agree well on the directionality of the change. Both observations show that the decrease in NAQFC emissions is insufficient to account for the NO_x change in this area. The annual changing rates from OMI and AQS are comparable to that (−5.3%/yr) derived from SCIAMACHY (Schneider and van der A, 2012), but significantly higher than that (−2.6%/yr) derived from a multi-instrument fitting (Hilboll et al., 2013).

5.1.7. Philadelphia

The NAQFC projection (−25%) is comparable to the observed decrease presented by OMI (−26%), but considerably smaller than that by AQS (−37%). Regardless of the large difference in the overall change, OMI and AQS agree well on the yearly trend across the period. The mean changing rates of NO_2 are −3.7%/yr, −5.3%/yr and −3.6%/yr from OMI, AQS and NAQFC, respectively.

5.1.8. Washington, DC

The overall change predicted by NAQFC is significantly smaller than the observations from both OMI and AQS. NAQFC estimates that emissions decrease by −28%, while OMI and AQS show −47% and −48% reductions during the same period. The yearly trends from OMI and AQS are also closely matched, in particular in the second half of the study period. The mean changing rates of NO_2 are −6.7%, −6.9% and −4.0% from OMI, AQS, and NAQFC, respectively. Different from trends in other cities, the AQS trend in Washington, DC displays a large reduction in the pre-recession period, and this decrease is even larger than the reduction during the recession. Further analysis of the AQS data shows that the pre-recession dive is caused by substantial changes at high NO_x sites from 2005 to 2007, which outweighs the changes from other sites with either lower NO_x levels or smaller changes (see Figure S5 in Supplemental Materials). In addition, there are variations in the data samples used to calculate the trend from AQS (Table 3).

5.2. Comparison of end-of-period change

Satellite NO_2 observations demonstrate the potential to reduce the time lag of NEIs (e.g., Lamsal et al., 2011), which is of particular interest to the air quality forecasting community (Tong et al., 2012). To this end, we compare here the overall NO_x changes among NAQFC, OMI, and AQS during the seven-year period (Table 1). From 2005 to 2012, the NAQFC emission updates estimate a NO_x reduction from −15% to −31% over the eight cities, with a mean reduction of −25%. For the same period, OMI shows NO_x changes from −24% to −47%, with a mean change of −35%, and the AQS changes range from −25% to −48%, with a mean of −38%. While the OMI change cannot be directly translated into emission changes in the NAQFC emissions dataset, as to be discussed in Section 6, the consistent temporal trends between OMI and NAQFC, together with the close match with the AQS ground observations, clearly suggest that even the substantial projected reductions used in the 2012 NAQFC emission updates have not yet captured the considerable emission reduction in these urban areas. This result is consistent with those presented by previous studies that have examined the NO_2 surface concentrations or column density from the NAQFC chemistry transport model (Chai et al., 2013; Pan et al., 2014). An earlier study by Kim et al. (2009), based on the Weather Research and Forecasting-Chemistry (WRF-Chem) model and NO_2 columns from SCIAMCHY and OMI, also found that model NO_2 columns over large urban areas along the US west coast are approximately twice as large as satellite retrievals. These large discrepancies in the surface concentrations, column density, and annual trend imply overestimates of NO_x emissions, particularly of mobile sources, over these cities. The US EPA reports the national NO_x emission trend in a national total and by emission sectors (US EPA, 2014a, 2014b). From 2005 to 2012, the EPA estimates that the total anthropogenic NO_x emissions have been reduced by 33%, with the largest decrease in the EGU sections by approximately 52%, followed by 35% from onroad engines, 31% from offroad engines, and 29% from industrial operations. Although it is difficult to directly compare these national trends with the city-wide trends derived in this study, the magnitude of estimated changes is consistent with those observed from OMI and AQS. The inclusion of these changes in future NEIs is expected to reduce emission uncertainties for atmospheric modeling, although the time lag between NEIs and forecasting years will remain.

The average annual NO_x change rate over 2005 to 2012 is −5.0%/yr from OMI and −5.3%/yr from AQS, both larger than the −3.6%/yr adopted by the NAQFC emission projections. These reduction rates are comparable to the −4.3%/yr over the Ohio River Valley observed by GOME and SCIAMACHY between 1997 and 2006 (Stavrakou et al., 2008). Such a trend is also supported by the analysis of nitrogen deposition data over rural and remote areas based on the Clean Air Status Trends Network and National Trends Network (Pinder et al., 2011), suggesting broad agreement of the large-scale NO_x changes across the entire region. This downward trend is significant among developed regions, where only a moderate to low reduction rate was detected by Stavrakou et al. (2008), and contrasts with the upward trend over developing regions (e.g., Asia) (Zhang et al., 2012). To accommodate such rapid emission changes in air quality models, it is important to increase the accuracy of NO_x emission data as many parts of the United States have transitioned or soon will transition into NO_x-sensitive chemical regimes (Duncan et al., 2010). Therefore, even the region with the world's finest emission data will face challenges updating the NO_x emission inventories more timely and accurately.

Table 1
Seven-year NO_x change according to NAQFC, OMI, and AQS in eight US cities from 2005 to 2012.

City	Atlanta	Boston	Dallas	Houston	Los Angeles	New York	Philadelphia	Washington, DC	Mean
OMI	−42%	−37%	−34%	−24%	−40%	−32%	−26%	−47%	−35%
AQS	−45%	−33%	−33%	−25%	−37%	−45%	−37%	−48%	−38%
NAQFC	−31%	−28%	−24%	−28%	−15%	−22%	−25%	−28%	−25%

Table 2
Comparisons of NO_x changes (%/yr) before, during, and after the 2008 economic recession in the eight urban centers as shown by OMI and AQS.

Stage	Sources	Atlanta	Boston	Dallas	Houston	Los Angeles	New York	Philadelphia	Washington, DC	Mean
Before	OMI SP	−11.7	−9.4	−7.5	−5.7	−3.3	−7.5	−0.6	−12.3	−7.3
	OMI BEHR	−10.1	−14.7	−5.9	−7.6	−5.5	−9.3	−9.4	−9.0	−8.9
	AQS	−9.9	−2.1	−5.2	0.7	−2.0	−5.5	−5.5	−18.7	−6.0
During	OMI SP	−5.5	−7.5	−8.9	−7.9	−13.1	−6.2	−11.7	−13.0	−9.2
	OMI BEHR	−13.5	0.3	−6.9	−7.7	−15.0	−10.5	−9.9	−9.9	−9.1
	AQS	−17.5	−7.0	−13.0	−14.0	−10.3	−13.6	−7.0	−3.7	−10.8
After	OMI SP	−6.0	−3.3	−2.1	0.4	−5.0	−3.2	−1.2	−2.3	−2.8
	OMI BEHR	4.1	−5.5	−1.7	0.3	−2.2	−9.2	−9.3	−5.6	−3.6
	AQS	1.4	−6.1	0.1	0.2	−6.4	−5.4	−6.1	−5.3	−3.4

Table 3
Data points of the NO_2 column density from OMI and NO_x concentrations from AQS during July from 2005 to 2012.

Year	City															
	Atlanta		Boston		Dallas		Houston		Los Angeles		New York		Philadelphia		Washington	
	OMI	AQS	OMI	AQS	OMI	AQS	OMI	AQS	OMI	AQS	OMI	AQS	OMI	AQS	OMI	AQS
2005	334	561	324	968	415	1403	362	1611	1479	1815	1263	762	332	498	327	426
2006	458	580	326	833	475	1232	293	1707	1467	1987	1462	669	354	580	428	394
2007	358	452	410	669	437	1233	35	1821	1775	1993	1299	530	337	441	321	872
2008	532	437	378	868	526	1276	443	1730	1590	1946	1419	687	353	458	341	719
2009	440	356	295	694	364	1225	441	1747	1460	1983	1332	682	376	237	370	782
2010	486	342	264	852	366	1524	259	1704	1458	1871	1659	566	463	336	438	791
2011	520	342	339	928	575	1604	470	1831	1459	1859	1605	326	380	357	347	688
2012	545	343	393	923	500	1155	284	1855	840	1680	1464	471	393	473	312	796

5.3. Impact of economic recession on NO_x emissions

In all cities examined in this study, we found that the first half of the period sees a greater NO_x reduction than the second half, perhaps because of the combined effects of emission control regulations and economic recession. In recent decades, regional and national emission control programs, such as the Ozone Transport Region (OTR) NO_x Cap and Allowance Trading Program, the NO_x State Implementation Plan (SIP) Call, and the Cross-State Air Pollution Rule (CSAPR), have been implemented that aim to reduce anthropogenic NO_x emissions from major sources in North America (Richter et al., 2005; Kim et al., 2009; Stavrakou et al., 2008; van der A et al., 2008; Konovalov et al., 2010; Russell et al., 2010). Similar trends have also been observed in other developed regions including Europe and Japan (van der A et al., 2008; Konovalov et al., 2010; Castellanos and Boersma, 2012). Meanwhile, economic development and increases in energy use have been associated with the observed rises in NO_x emissions over developing countries (van der A et al., 2008; Zhou et al., 2012). The impact of the 2008 global economic recession on US NO_x emissions was examined by Russell et al. (2012) using OMI Berkeley High Resolution (BEHR) product. They found that the decreases in urban NO_2 column densities accelerated during the recession, changing from −6%/yr beforehand to −8%/yr during the financial crisis, and then slowing to −3%/yr thereafter (Russell et al., 2012). Satellite and ground observations were also used to quantify the impact of the economic recession on air quality in Greece (Vrekoussis et al., 2013) and pollution emissions from marine shipping lanes (de Ruyter de Wildt et al., 2012). Collectively, these studies demonstrate that it is possible to use satellite observations to detect the effect of short-term economic fluctuations on NO_x emissions.

Following the definition of Russell et al. (2012), we divide the seven-year study period into three stages in order to examine the NO_x rates of change before (2005–2007), during (2008–2009), and after (2010–2012) the economic recession. Table 2 shows the yearly NO_x rates of change for each subperiod. In addition to the OMI Standard Product (OMI SP) and AQS data used here, we also include in Table 2 the results extracted from OMI BEHR (Russell et al., 2012) for comparison purposes. Table 2 shows considerable variability in the magnitude of NO_x changes from city to city. The AQS data clearly display larger reduction rates during the recession than before the recession in all cities except Washington DC. The OMI data also show larger reduction during the recession in five of the eight cities, but the reduction rate is generally smaller than that from the AQS data. In the other three cities (Atlanta, Boston, and New York), the reduction rate from OMI was actually smaller during recession than before recession, different from that by AQS. By comparison the rates of change derived from the OMI BEHR data are different from those derived from OMI SP. The difference in the NO_2 trends between the two OMI products is attributed to several factors, including retrieval approaches, data filtering criteria, and spatial and temporal coverage. In particular, Russell et al. (2012) derived the BEHR OMI trends using 12-month data, while this study is limited to the July data. The temporal coverage affects not only the size of data samples, but also other relevant factors such as the relative contribution of local emissions and regional transport to NO_2 columns since the lifetime of NO_2 is shorter in July than in cold seasons. In summary, there are inconsistencies in the detailed trends before, during and after recession at the city level. Future work is needed to extend this study beyond July to examine if such response to economic recession also exists in other months. While the OMI SP data are used here to exemplify the feasibility of using satellite data to validate emission updates, other NO_2 products (such as BEHR, DOMINO and GOME2) should be considered in the future to obtain a broader view of the emission trends.

6. Discussion of uncertainties

There are several factors contributing to the uncertainties in the three-member intercomparisons presented in Fig. 6. These factors include data quality in AQS and OMI data, uncertainties in NO_x emission model data, representativeness of NO_x life cycles by different datasets, and mismatched sampling time between OMI and AQS. We discuss below how these factors may affect the

interpretation of the trend comparison. The trend data derived from both OMI and AQS have gone through rigorous quality filtering as described Sections 2.3. However, the quality filtering procedures also affect the completeness of individual dataset. For OMI, the criteria applied to screen NO_2 data by cloudiness and row anomaly flag will reduce the size of data samples, resulting in varying data points eventually used to represent the OMI trend. Similarly, instrumental malfunctioning and other errors could lead to loss of valid data points from the AQS network. Table 3 lists the numbers of OMI and AQS data points used to derive the NO_x trends in each city. There are noticeable variations in the number of data points from both datasets. For instance, over Atlanta, there are fewer valid data points from OMI, but more from AQS during 2005–2007. The change in data samples is likely a cause of the discrepancy between the OMI and AQS trends in Fig. 6a. There are a large number of data points excluded (due to clouds) from OMI in 2006 and 2007 over Houston, which could be responsible for the difference between the OMI trend and that from AQS and NAQFC (Fig. 6d). There are a smaller number of AQS observations in 2005 and 2006 over Washington, DC. that likely contributes to the large decrease between 2005 and 2008 over this area (Fig. 6f). Regardless of the large variations in data samples, both datasets reveal consistent downward NO_x trends, suggesting a certain level of representativeness of the validated data samples, although it is difficult to quantitatively assess the uncertainties caused by the missing data.

The NO_x trends examined here were obtained from three data sources that represent different aspects of the NO_x life cycle. OMI observes NO_2 column density in the troposphere, AQS monitors NO_x concentrations at the surface, and NEI describes the vertical flux rate immediately after being released into the atmosphere. Complicated processes including chemical transformation, transport, and deposition alter the relationships among these NO_x variables, making the direct comparison of their values extremely challenging. Our approach in this study compares the interannual trends derived from individual datasets, thereby minimizing the interference of certain factors affecting the relationships among them. Even so, some remaining issues must be recognized when interpreting our results, including the varying relationships among NO_x emissions, surface concentration, the atmospheric column, and the mismatched "sampling" time.

One of the concerns about the intercomparison is that the relationship between NO_2 column and NO_x emissions varies over space and time, making it challenging directly comparing the two parameters (Lamsal et al., 2011). Most urban centers examined in this study are in NO_x-saturated chemical regimes (e.g., Tong et al., 2006; Duncan et al., 2010). Enhanced near-source deposition and chemical destruction occur when dense NO_x emissions are confined in urban plumes, where the limited availability of and mixing with volatile organic compounds constrains the preservation of emitted NO_x in the atmosphere (Ryerson et al., 1998). As NO_x emissions decrease over time, the chemical regime and near-source removal change, and this change subsequently affects the relationships among emissions, ambient concentration, and vertical column through a chain of chemical and photochemical reactions (Warneck, 2000). One of these relationships is the local sensitivity of NO_2 column change to changes in NO_x emissions, represented by β in the following equation (Lamsal et al., 2011):

$$\Delta E/E = \beta \times \Delta\Omega/\Omega \quad (2)$$

where $\Delta\Omega$ is the column change driven by the change in emissions ΔE. In order to directly compare the trends from OMI and NAQFC or other emission inventories, it is necessary to assume that the change in β over one metropolitan area is small enough for this factor to be canceled out when deriving the long-term trend. The overall difference in these trends is a combination of the changes in NO_x emissions, columns, and their relative sensitivity. For example, by using the global chemical transport model GEOS-Chem, Lamsal et al. (2011) found that a perturbation of 30% only changes β by <2%. Therefore, the overall error caused by non-uniformity of β is expected to be small compared with the NO_x trends, since the annual NO_x change over a city is relatively small (−5%) and the seven-year changes are approximately 30% in most cases (Table 1). Our own simulations with the NAQFC CMAQ model showed a similar magnitude of sensitivities between NO_x emissions and the NO_2 column.

Another concern about the intercomparison is that different sampling times were used for different datasets. The NAQFC emission model uses a diurnal profile to split total NO_x emissions into hourly data, meaning that sampling time does not alter the relative change or trend. There is, however, a mismatch in the temporal resolutions between AQS and OMI. AQS samples NO_x concentrations hourly, while OMI observes the NO_2 column only once a day. In this study, we used early morning rush-hour data to derive the NO_x trend from NAQFC and AQS, but early afternoon data for the OMI trend. It thus remains unclear if the difference in sampling time affects the derived NO_x trends. To examine this issue, we repeated the AQS data analysis, but by using the early afternoon hours covering the OMI passing time (12–3 pm local time). We then compared the annual trends in AQS in both early morning and early afternoon with the OMI data in order to examine the difference between the two AQS datasets as well as between the AQS and OMI observations (Fig. 7). Compared with the early morning data, the afternoon AQS data display larger year-to-year variability, particularly over Atlanta, Boston, and Dallas. In other cities, the difference is smaller. For all cities, there is a consistent downward trend during this period, and the trend is generally in accord with the OMI trend. Between the morning and afternoon AQS trends, the former is better correlated with the OMI trend, perhaps because of the stronger dominance of local emissions and weaker interference of meteorology and photochemistry in early morning and the locality of surface sites (Steinbacher et al., 2007). This is consistent with an earlier NO_x budget study using a modeling technique called budget process analysis (Tong et al., 2005) which shows that NO_x budget is largely controlled by chemistry and transport even in rural area where emissions and chemical processes are less vibrant as in urban areas. The better agreement between OMI and early morning AQS data, however, does not necessarily imply that early morning is an ideal time window for space-based observations, since surface concentration and column density display distinct responsiveness to the chemical and physical processes affecting the NO_x life cycle. Unfortunately reliable fine-resolution satellite and ground NO_2 data are not available, which limits comparison of NO_x trends from different observations.

7. Conclusion and recommendations

This study derives multi-year NO_x trends from satellite and ground observations and uses these data to evaluate the emission updates for the US NAQFC predictions. Over the eight US cities examined here, both OMI and AQS show substantial downward trends from 2005 to 2012. The NO_x emission projection adopted by NAQFC tends to be in the right direction with the observed NO_x trend, but at a slower reduction rate (−25% in seven years vs. about −35% from OMI -38% from AQS), perhaps because of unaccounted effects of the 2008 economic recession in the NAQFC emissions. Both OMI and AQS datasets display distinct emission reduction rates before, during, and after the 2008 global recession

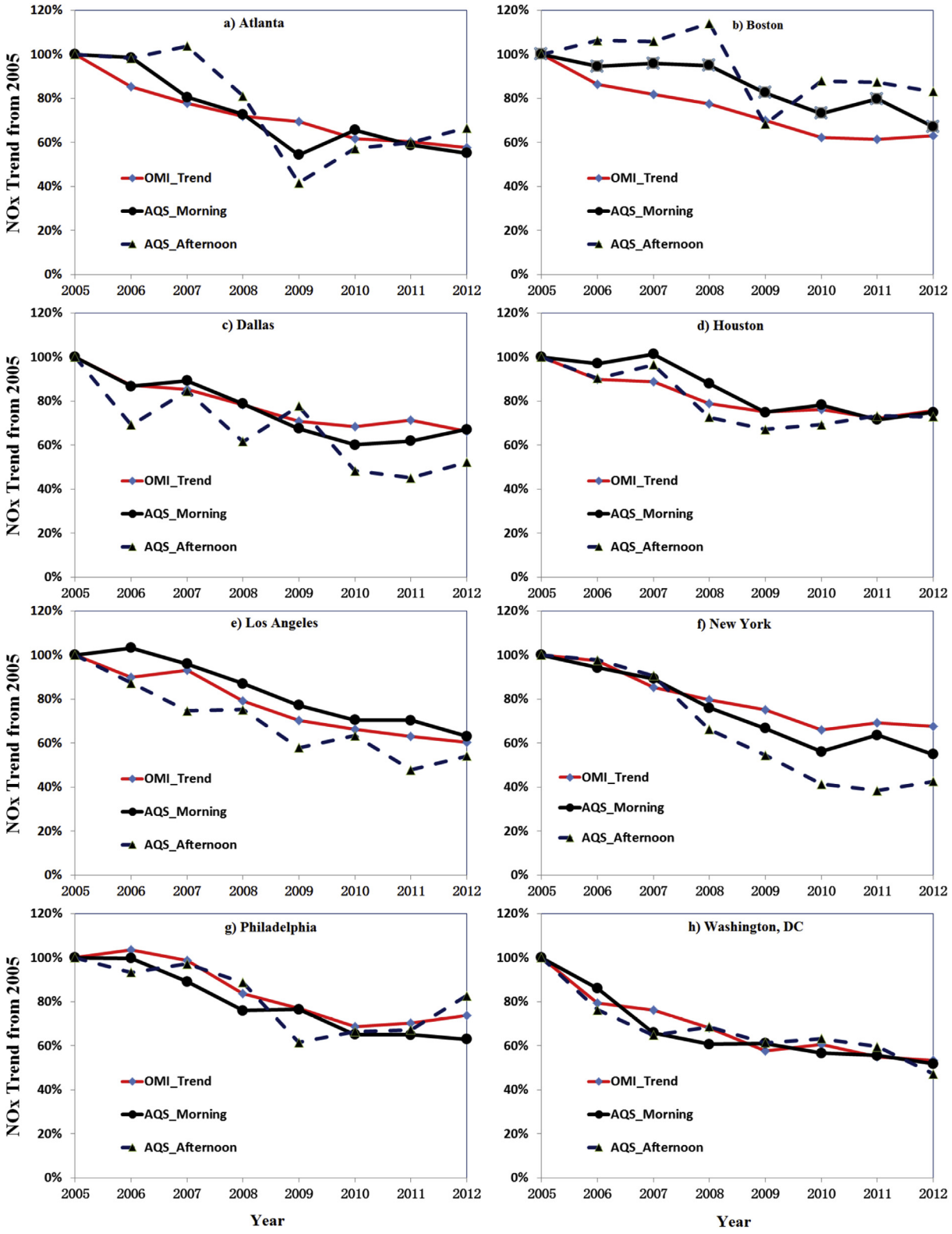

Fig. 7. Comparison of OMI NO_2 trend with NO_x trends derived from AQS during early morning (6–9 am local time) and early afternoon (12–3 pm) from 2005 to 2012 over eight cities: a) Atlanta, b) Boston, c) Dallas, d) Houston, e) Los Angeles, f) New York, g) Philadelphia, and h) Washington, DC.

in several cities, but the detailed changing rates are not necessarily consistent between the OMI and AQS data. NAQFC predictions of surface ozone concentrations were shown to have improved following the update for NO_x emissions in year 2012.

This study demonstrates the feasibility of using space and ground observations to objectively evaluate major updates of emission inventories, which are crucial to predict air quality accurately. It is interesting to note that the OMI-based NO_2 trend closely

matches the AQS ground observations of not only the overall reduction, but also the gradual series of NO_x changes. Given the wide spatial coverage and near real-time data availability, satellite NO_2 observations thus show a great potential to improve the quality of NO_x emission inventories used by time-sensitive applications, as suggested in earlier studies (Lamsal et al., 2011; Tong et al., 2012; Streets et al., 2013). Ground NO_x observations, particularly the morning rush-hour data, are another valuable data source that can be used in order to evaluate and improve emission inventories, although the monitors are mostly confined in urban areas. The combination of satellite, ground observations, and in-situ measurements (e.g., the CEM data in Frost et al., 2006) is likely to provide more reliable estimates of NO_x emissions and their trends, which is an issue of increasing importance as many urban areas in the US are transitioning to NO_x-sensitive chemical regimes with continuous emission reductions. It is also desirable to develop an emission data assimilation capability that allows timely ingestion of these observational data in order to address major emission uncertainties (e.g., Tong et al., 2012) in time-sensitive applications such as air quality forecasting.

Acknowledgments

This work has been supported by the NOAA JPSS Proving Ground and Risk Reduction Program (NA12NES4400007) and the NASA Earth Science Program through the National Climate Indicator (NNX13A045G) and Air Quality Applied Science Team initiatives. The authors are grateful to Dr. Bryan Duncan at NASA and two anonymous reviewers for their constructive comments.

Appendix A. Supplementary data

Supplementary data related to this article can be found at http://dx.doi.org/10.1016/j.atmosenv.2015.01.035.

References

Boersma, K.F., Eskes, H.J., Brinksma, E.J., 2004. Error analysis for tropospheric NO_2 retrieval from space. J. Geophys. Res. 109, D04311. http://dx.doi.org/10.1029/2003JD003962.

Boersma, K.F., Eskes, H.J., Veefkind, J.P., Brinksma, E.J., van der A, R.J., Sneep, M., van den Oord, G.H.J., Levelt, P.F., Stammes, P., Gleason, J.F., Bucsela, E.J., 2007. Near-real time retrieval of tropospheric NO_2 from OMI. Atmos. Chem. Phys. 7, 2103–2118. http://dx.doi.org/10.5194/acp-7-2103-2007.

Bond, T.C., Streets, D.G., Yarber, K.F., Nelson, S.M., Woo, J.-H., Klimont, Z., 2004. A technology-based global inventory of black and organic carbon emissions from combustion. J. Geophys. Res. 109, D14203. http://dx.doi.org/10.1029/2003JD003697.

Bucsela, E.J., Krotkov, N.A., Celarier, E.A., Lamsal, L.N., Swartz, W.H., Bhartia, P.K., Boersma, K.F., Veefkind, J.P., Gleason, J.F., Pickering, K.E., 2013. A new stratospheric and tropospheric NO_2 retrieval algorithm for nadir-viewing satellite instruments: application to OMI. Atmos. Meas. Tech. 6, 2607–2626.

Byun, D., Schere, K.L., 2006. Review of the governing equations, computational algorithms, and other components of the models-3 community multiscale air quality (CMAQ) modeling system. Appl. Mech. Rev. 55, 51–77.

Castellanos, P., Boersma, K.F., 2012. Reductions in nitrogen oxides over Europe driven by environmental policy and economic recession. Sci. Reports 2 (265), 1–7. http://dx.doi.org/10.1038/srep00265.

Chai, T., Kim, H.-C., Lee, P., Tong, D., Pan, L., Tang, Y., Huang, J., McQueen, J., Tsidulko, M., Stajner, I., 2013. Evaluation of the United States National Air Quality Forecast Capability experimental real-time predictions in 2010 using Air Quality System ozone and NO_2 measurements. Geosci. Model Dev. 6, 1831–1850. http://dx.doi.org/10.5194/gmd-6-1831-2013.

Choi, Y., Kim, H., Tong, D., Lee, P., 2012. Summertime weekly cycles of observed and modeled NO_x and O_3 concentrations as a function of satellite-derived ozone production sensitivity and land use types over the Continental United States. Atmos. Chem. Phys. 12, 6291–6307. http://dx.doi.org/10.5194/acp-12-6291-2012.

Crutzen, P.J., Gidel, L.T., 1983. A two-dimensional photochemical model of the atmosphere, 2, the tropospheric budgets of the anthropogenic chlorocarbons CO, CH_4, CH_3C1 and the effect of various NO_x sources on tropospheric ozone. J. Geophys. Res. 88, 6641–6661.

de Ruyter de Wildt, M., Eskes, H., Boersma, K.F., 2012. The global economic cycle and satellite-derived NO_2 trends over shipping lanes. Geophys. Res. Lett. 39, L01802. http://dx.doi.org/10.1029/2011GL049541.

Dobber, M.R., Braak, R., 2010. Known Instrumental Affects that Affect the OMI L1B Product of the Ozone Monitoring Instrument on EOS Aura. Last update: 17 December 2010. http://disc.sci.gsfc.nasa.gov/Aura/data-holdings/OMI/documents/v003/known_instrumental_effects_l1b_data_omi_v6.pdf.

Duncan, B., Yoshida, Y., Olson, J., Sillman, S., Retscher, C., Martin, R., Lamsal, L., Hu, Y., Pickering, K., Retscher, C., Allen, D., Crawford, J., 2010. Application of OMI observations to a space-based indicator of NO_x and VOC controls on surface ozone formation. Atmos. Environ. 44, 2213–2223. http://dx.doi.org/10.1016/j.atmosenv.2010.03.010.

Duncan, B., Yoshida, Y., de Foy, B., Lamsal, L., Streets, D., Lu, Z., Pickering, K., Krotkov, N., 2013. The observed response of Ozone Monitoring Instrument (OMI) NO_2 columns to NO_x emission controls on power plants in the United States: 2005-2011. Atmos. Environ. 81, 102–111. http://dx.doi.org/10.1016/jatmosenv.2013.08.068.

Dunlea, E.J., Herndon, S.C., Nelson, D.D., Volkamer, R.M., San Martini, F., Sheehy, P.M., Zahniser, M.S., Shorter, J.H., Wormhoudt, J.C., Lamb, B.K., Allwine, E.J., Gaffney, J.S., Marley, N.A., Grutter, M., Marquez, C., Blanco, S., Cardenas, B., Retama, A., Ramos Villegas, C.R., Kolb, C.E., Molina, L.T., Molina, M.J., 2007. Evaluation of nitrogen dioxide chemiluminescence monitors in a polluted urban environment. Atmos. Chem. Phys. 7, 2691–2704. http://dx.doi.org/10.5194/acp-7-2691-2007.

Eder, B., Kang, D., Mathur, R., Pleim, J., Yu, S., Otte, T., Pouliot, G., 2009. A performance evaluation of the National Air Quality Forecast Capability for the summer of 2007. Atmos. Environ. 43, 2312–2320.

Frost, G.J., et al., 2006. Effects of changing power plant NOx emissions on ozone in the eastern United States: proof of concept. J. Geophys. Res. 111, D12306. http://dx.doi.org/10.1029/2005JD006354.

Godowitch, J.M., Pouliot, G., Rao, S.T., 2010. Assessing multi-year changes in modeled and observed urban NO_x concentrations from a dynamic model evaluation perspective. Atmos. Environ. 44 (24), 2894–2901.

Granier, C., et al., 2011. Evolution of anthropogenic and biomass burning emissions of air pollutants at global and regional scales during the 1980–2010 period. Clim. Change 109, 163–190.

Harley, R.A., Marr, L.C., Lehner, J.K., Giddings, S.N., 2005. Changes in motor vehicle emissions on diurnal to decadal time scales and effects on atmospheric composition. Environ. Sci. Tech. 39, 5356–5362.

Hilboll, A., Richter, A., Burrows, J.P., 2013. Long-term changes of tropospheric NO_2 over megacities derived from multiple satellite instruments. Atmos. Chem. Phys. 13, 4145–4169.

Houyoux, M.R., Vukovich, J.M., Coats Jr., C.J., Wheeler, N.J.M., Kasibhatla, P.S., 2000. Emission inventory development and processing for the seasonal model for Regional Air Quality (SMRAQ) Project. J. Geophys. Res. 105 (D7), 9079–9090.

Hudman, R.C., Moore, N.E., Mebust, A.K., Martin, R.V., Russell, A.R., Valin, L.C., Cohen, R.C., 2012. Steps towards a mechanistic model of global soil nitric oxide emissions: implementation and space based-constraints. Atmos. Chem. Phys. 12, 7779–7795. http://dx.doi.org/10.5194/acp-12-7779-2012.

Jerrett, M., Burnett, R.T., Pope III, C.A., Ito, K., Thurston, G., Krewski, D., et al., 2009. Long-term ozone exposure and mortality. N. Engl. J. Med. 360, 1085–1095.

Kang, D., Mathur, R., Rao, S.T., 2010. Real-time bias-adjusted O_3 and $PM_{2.5}$ air quality index forecasts and their performance evaluations over the continental United States. Atmos. Environ. 44, 2203–2212.

Kim, S.W., Heckel, A., Frost, G.J., Richter, A., Gleason, J., Burrows, J.P., McKeen, S., Hsie, E.Y., Granier, C., Trainer, M., 2009. NO_2 columns in the western United States observed from space and simulated by a regional chemistry model and their implications for NO_x emissions. J. Geophys. Res. 114, D11301. http://dx.doi.org/10.1029/2008JD011343.

Konovalov, I.B., Beekmann, M., Richter, A., Burrows, J.P., Hilboll, A., 2010. Multi-annual changes of NO_x emissions in megacity regions: nonlinear trend analysis of satellite measurement based estimates. Atmos. Chem. Phys. 10, 8481–8498. http://dx.doi.org/10.5194/acp-10-8481-2010.

Lamsal, L.N., Martin, R.V., Padmanabhan, A., van Donkelaar, A., Zhang, Q., Sioris, C.E., Chance, K., Kurosu, T.P., Newchurch, M.J., 2011. Application of satellite observations for timely updates to global anthropogenic NO_x emission inventories. Geophys. Res. Lett. 38, L05810. http://dx.doi.org/10.1029/2010GL046476.

Lamsal, Lok N., Duncan, Bryan N., Yoshida, Yosuko, Krotkov, Nickolay A., Pickering, Kenneth E., Streets, David G., Lu, Zifeng, 2015. U.S. NO_2 trends (2005–2013): EPA Air Quality System (AQS) data versus improved observations from the Ozone Monitoring Instrument (OMI). Atmos. Environ (submitted for publication).

Lee, P., Fong, N., 2011. Coupling of important physical processes in the planetary boundary layer between meteorological and chemistry models for regional to Continental scale air quality forecasting: an overview. Atmosphere 2 (3), 464–483.

Levelt, P.F., van den Oord, G.H.J., Dobber, M.R., Mälkki, A., Visser, H., de Vries, J., Stammes, P., Lundell, J.O.V., Saari, H., 2006. The ozone monitoring instrument. IEEE Trans. Geosci. Remote Sens. 44, 1093–1101. http://dx.doi.org/10.1109/TGRS.2006.872333.

Liu, S.C., Trainer, M., Fehsenfeld, F., Parrish, D.D., Williams, E.J., Fahey, D.W., Htibler, G., Murphy, P.C., 1987. Ozone production in the rural troposphere and the implications for regional and global ozone distributions. J. Geophys. Res. 92, 4191–4207.

Martin, R.V., et al., 2002. An improved retrieval of tropospheric nitrogen dioxide from GOME. J. Geophys. Res. 107 (D20), 4437. http://dx.doi.org/10.1029/

2001JD001027.
Martin, R.V., Jacob, D.J., Chance, K., Kurosu, T.P., Palmer, P.I., Evans, M.J., 2003. Global inventory of nitrogen oxide emissions constrained by space-based observations of NO_2 columns. J. Geophys. Res. 108 (D17), 4537. http://dx.doi.org/10.1029/2003JD003453.
McClenny, W.A., Williams, E.J., Cohen, R.C., Stutz, J., 2002. Preparing to measure the effects of the NO_x SIP call — methods for ambient air monitoring of NO, NO_2, NO_y, and individual NO_z species. J. Air Waste Manage. Assoc. 52, 542–562.
Mijling, B., van derA, R.J., 2012. Using daily satellite observations to estimate emissions of short-lived air pollutants on a mesoscopic scale. J. Geophys. Res. 117, D17302. http://dx.doi.org/10.1029/2012JD017817.
Oetjen, H., Baidar, S., Krotkov, N.A., Lamsal, L.N., Lechner, M., Volkamer, R., 2013. Airborne MAX-DOAS measurements over California: testing the NASA OMI tropospheric NO_2 product. J. Geophys. Res. 118, 13. http://dx.doi.org/10.1002/jdrd.50550.
Otte, T.L., et al., 2005. Linking the Eta model with the Community Multiscale Air Quality (CMAQ) modeling system to build a national air quality forecasting system. Weather Forecast. 20, 367–384.
Pan, L., Tong, D.Q., Lee, P., Kim, H., Chai, T., 2014. Assessment of NO_x and O_3 forecasting performances in the U.S. National Air Quality Forecasting Capability before and after the 2012 major emissions updates. Atmos. Environ. 95, 610–619.
Pinder, R.W., Appel, K.W., Dennis, R.L., 2011. Trends in atmospheric reactive nitrogen for the Eastern United States. Environ. Pollut. 159, 3138–3141.
Platt, U., 1994. Differential optical absorption spectroscopy (DOAS). Chem. Anal. Ser. 127, 27–83.
Pope III, C.A., Burnett, R.T., Thun, M.J., Calle, E.E., Krewski, D., Ito, K., Thurston, G.D., 2002. Lung cancer, cardiopulmonary mortality, and long-term exposure to fine particulate air pollution. J. Am. Med. Assoc. 12, 1132–1141. http://dx.doi.org/10.1001/jama.287.9.1132.
Richter, A., Burrows, J.P., Nüβ, H., Granier, C., Niemeier, U., 2005. Increase in tropospheric nitrogen oxide over China observed from space. Nat. Lett. 437, 129–132. http://dx.doi.org/10.1038/nature04092.
Russell, A.R., Valin, L.C., Buscela, E.J., Wenig, M.O., Cohen, R.C., 2010. Space-based constraints on spatial and temporal patterns in NO_x emissions in California, 2005–2008. Environ. Sci. Technol. 44, 3607–3615.
Russell, A.R., Valin, L.C., Cohen, R.C., 2012. Trends in OMI NO_2 observations over the United States: effects of emission control technology and the economic recession. Atmos. Chem. Phys. 12, 12197–122209. http://dx.doi.org/10.5194/acp-12-12197-2012.
Ryerson, T.B., et al., 1998. Emissions lifetimes and ozone formation in power plant plumes. J. Geophys. Res. 103 (D17), 22569–22583. http://dx.doi.org/10.1029/98JD01620.
Schneider, P., van der A, R.J., 2012. A global single-sensor analysis of 2002–2011 tropospheric nitrogen dioxides trends observed from space. J. Geophys. Res. 117, D16309. http://dx.doi.org/10.1029/2012JD017571.
Spicer, C.W., 1983. Smog chamber studies of NO_x transformation rate and nitrate/precursor relationships. Environ. Sci. Technol. 17, 112–120.
Stajner, I., Davidson, P., Byun, D., McQueen, J., Draxler, R., Dickerson, P., Meagher, J., 2012. US national air quality forecast capability: expanding coverage to include particulate matter. In: Steyn, Douw G., Castelli, Silvia Trini (Eds.), NATO/ITM Air Pollution Modeling and its Application, vol. XXI. Springer, Netherlands, pp. 379–384. http://dx.doi.org/10.1007/978-94-007-1359-8_64.
Stavrakou, T., Muller, J.F., Boersma, K.F., De Smedt, I., van der A, R.J., 2008. Assessing the distribution and growth rates of NO_x emission sources by inverting a 10-year record of NO_2 satellite columns. Geophys. Res. Lett. 35, L10801. http://dx.doi.org/10.1029/2008GL033521.
Steinbacher, M., Zellweger, C., Schwarzenbach, B., Bugmann, S., Buchmann, B., Ordòñez, C., Prevot, A.S.H., Hueglin, C., 2007. Nitrogen oxides measurements at rural sites in Switzerland: bias of conventional measurement techniques. J. Geophys. Res. D11307. http://dx.doi.org/10.1029/2006JD007971.
Streets, D.G., et al., 2013. Emissions estimation from satellite retrievals: a review of current capability. Atmos. Environ. 77, 1011–1042.
Tong, D.Q., Mauzerall, D.L., 2006. Spatial variability of summertime tropospheric O3 in the continental United States: an evaluation of the CMAQ model and its implications. Atmos. Environ. 40, 3041.
Tong, D.Q., Kang, D., Viney, P.A., Rayb, J.D., 2005. Reactive Nitrogen Oxides in the Southeast United States National Parks: Source Identification.
Tong, D.Q., Muller, N., Mauzerall, D.L., Mendelsohn, R., 2006. An integrated assessment of the impacts of ozone resulting from nitrogen oxide emissions near Atlanta. Environ. Sci. Technol. 40 (5), 1395.
Tong, D.Q., Mathur, R., Schere, K., Kang, D., Yu, S., 2007. The use of air quality forecasts to assess impacts of air pollution on crops: a case study of assessing soybean yield losses from ozone in the United States. Atmos. Environ. 41 (38), 8772–8784.
Tong, D.Q., Mathur, R., Kang, D., Yu, S., Schere, K.L., Pouliot, G., 2009. Vegetation exposure to ozone over the continental United States: assessment of exposure indices by the Eta-CMAQ air quality forecast model. Atmos. Environ. 43 (3), 724–733.
Tong, D.Q., Lee, P., Saylor, R.D., 2012. New Direction: the need to develop process-based emission forecasting models. Atmos. Environ. 47, 560–561.
US DOE, 2012. Annual Energy Outlook 2012. DOE Energy Information Agency (EIA). Document No. DOE/EIA-0383(2012). Accessed online Nov 18, 2012 at. http://www.eia.gov/forecasts/aeo/pdf/0383(2012).pdf.
US EPA, 2011. Technical Support Document (TSD) for the Final Transport Rule. Docket ID No. EPA-HQ-OAR-2009-0491 (accessed online Nov 18, 2012 at. http://www.epa.gov/airtransport/pdfs/EmissionsInventory.pdf.
US EPA, 2014a. The Green Book Nonattainment Areas for Criteria Pollutants. Available online at: http://www.epa.gov/airquality/greenbook/index.html (accessed on 10.02.14.).
US EPA, 2014b. 1970–2013 Average Annual Emissions, from National Emission Inventory (NEI) Air Pollutant Trends Data. Available online at: http://www.epa.gov/ttn/chief/trends/trends06/national_tier1_caps.xlsx (accessed on 10.02.14.).
van der A, R.J., Eskes, H.J., Boersma, K.F., van Noije, T.P.C., Van Roozendael, M., De Smedt, I., Peters, D.H.M.U., Meijer, E.W., 2008. Trends, seasonal variability and dominant NO_x source derived from a ten year record of NO_2 measured from space. J. Geophys. Res. 113, D04302. http://dx.doi.org/10.1029/2007JD009021.
Vrekoussis, M., Richter, A., Hilboll, A., Burrows, J.P., Gerasopoulos, E., Lelieveld, J., Barrie, L., Zerefos, C., Mihalopoulos, N., 2013. Economic crisis detected from space: air quality observations over Athens/Greece. Geophys. Res. Lett. 40, 458–463. http://dx.doi.org/10.1002/grl.50118.
Warneck, P., 2000. Chemistry of the Natural Atmosphere, Second ed. Academic Press, ISBN 0-12-735632-0.
Zhang, Q., Geng, G.N., Wang, S.W., Richter, A., He, K.B., 2012. Satellite remote sensing of changes in NO_x emissions over China during 1996–2010, Chinese. Sci. Bull. 57, 2857–2864.
Zhou, Y., Brunner, D., Hueglin, C., Henne, S., Staehelin, J., 2012. Changes in OMI tropospheric NO_2 columns over Europe from 2004 to 2009 and the influence of meteorological variability. Atmos. Environ. 46, 482–495.